

A finite element model to predict axial forces with friction in tubing strings

Otávio B. A. Rodrigues¹, Catarina N. A. Fernandes¹, João P. N. Araújo¹, William W. M. Lira¹, João P. L. Santos¹, Charlton O. Souza²

¹Laboratory of Scientific Computing and Visualization, Federal University of Alagoas
Avenida Lourival Melo Mota, S/N, Tabuleiro do Martins, 57072-970, Maceió/Alagoas, Brazil
otavio.rodrigues@lccv.ufal.br, catarina@lccv.ufal.br, joaopna@lccv.ufal.br, william@lccv.ufal.br, jpls@lccv.ufal.br
²Petróleo Brasileiro, CENPES
Avenida Horácio de Macedo, 950, Cidade Universitária, 21941-915, Rio de Janeiro/Rio de Janeiro, Brazil
charlton@petrobras.com.br

Abstract. This work shows a one-dimensional finite element model to predict axial forces with friction in tubing strings subjected to operational loads in the production of oil and gas. These strings undergo several combinations of axial forces throughout their lifetime. Accurate prediction of these forces is essential to maintain the structural integrity of this fundamental component of the well barrier system. Frictional forces, which impact axial forces, occur due to the contact between the string and the casing, which happens when the tube buckles. Due to the variety of operational loads, a general solution to the friction problem requires a numerical approach. To achieve the proposed objective, the adopted modelling is verified through analytical solutions, investigating the results related to the axial forces and displacements undergone by the tubing during a specific operation. Mesh refinement studies and computational cost of the simulations are also discussed in a case study. It is observed a good concordance between numerical results, and an acceptable computational cost. The main contribution of the work is the possibility of using numerical modelling for tubing, including friction, with good accuracy, low computational cost, and potential for real-time analysis.

Keywords: Tubing, Friction, Axial forces, Finite elements

1 Introduction

It is crucial to understand that operational loads on tubing strings can significantly impact their integrity. Well integrity assessment regulations outline specific load cases to consider, such as oil production and fluid injection. Bellarby [1] emphasizes the need to prioritize the assessment of the most critical cases concerning axial forces based on the defined loadings.

Self-weight, temperature, pressures, buckling, and friction influence axial forces during operations in tubing strings. Buckling and friction are directly related since this instability creates a contact force between the tubing and casing strings. This contact force, known as friction force, transforms into axial forces. Mitchell [2] explains that friction due to buckling has analytical solutions limited to specific loads, thus necessitating numerical methods for general solutions.

Bellarby [1] states that when dealing with operational loads, it is common to initially disregard friction. This is because these loads are applied over a period that can last years, the displacements are relatively small, and the effects of vibrations tend to alleviate contact and friction forces. However, it is important to acknowledge that the complete absence of friction cannot be guaranteed; therefore, it is necessary to conduct an analysis sensitive to the presence of friction. In these analyses, the models are constructed initially without friction, and later a realistic friction factor is introduced.

Friction impacts operational loads, especially during buckling, and is influenced by the load history, as mentioned by Mitchell [3]. It is crucial to note that friction, though often underestimated, plays a significant role in buckling analysis [4].

Several studies have explored the effects of friction between the tubing and casing strings on axial forces, including those presented by Brett et al. [5], Wu and Juvkam-Wold [6], and Miska et al. [7]. However, these studies do not account for load history in their friction analyses. As mentioned earlier, load history directly influences

the resulting axial forces because the string's kinematics define the direction of movement and friction. Models presented by Mitchell [2] and Mitchell et al. [8] incorporate this load history.

Among studies that support load history, Mitchell [2] stands out for its static numerical modelling. This model features a cubic displacement field and dependent degrees of freedom for the finite element in terms of displacement and elastic axial strain. These aspects introduce complexities, such as the piston effect from composite sections in the string or intermediate packers. This effect creates discontinuities in axial strains and axial forces, requiring a special transition element, as noted by Mitchell [2].

Mitchell [2] did not explore the application of the transition element in his work. However, Rodrigues [9] builds on this modelling to create a simplified strategy. He added small elements before and after diameter changes to capture discontinuities. This approach worked well but required filtering to remove noise from the results.

Based on these considerations, this work proposes a finite element model based on Mitchell [2], but considering only displacement degrees of freedom to predict axial loads with friction in tubing strings under operational loads. To achieve the proposed goal, the study examines elements with linear, quadratic, and cubic displacement fields. First, it implements and verifies these elements using a classic example with a known analytical solution. Then, it investigates a synthetic yet realistic well. The study compares forces, axial displacements, and computational costs between the proposed and reference models through mesh refinement analyses. The main contribution of this work is the use of numerical modelling for tubing with potential application in real-time analysis.

2 Numerical modelling of friction due to buckling

Mitchell [2] proposes that the axial force in the tubular varies with depth due to the effects of self-weight and friction generated by buckling, as illustrated and generalized through the equation in Fig. 1.

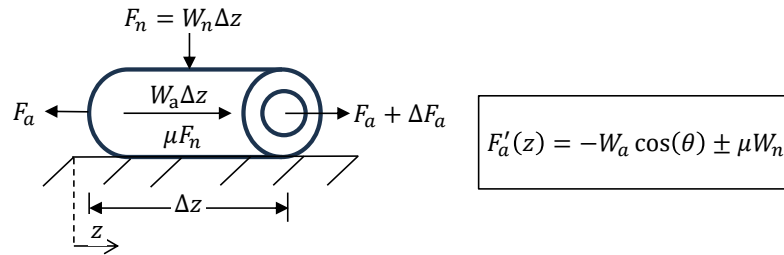


Figure 1. Tubing force balance including friction.

In this Figure, $F'_a(z)$ is the derivative of the axial force with respect to the depth z , W_a is the weight per unit length of the string, μ is the friction coefficient, W_n is the contact force due to buckling, and θ is the inclination of the well relative to the vertical.

Using the static equilibrium and constitutive equations of a linear elastic material, it is possible to define the axial force F_a as

$$F_a = EA_s \varepsilon_z - \nu A_s (\sigma_r + \sigma_\theta), \quad (1)$$

where E is the Young modulus, A_s is the tubular steel cross-sectional area, ε_z is the axial strain, ν is the Poisson coefficient, σ_r is the radial stress, and σ_θ is the hoop stress. Tubing strings undergo thermal effects that can cause either elongation or shortening. Thus, the string undergoes a thermal deformation ε_T defined as

$$\varepsilon_T = K \Delta T, \quad (2)$$

where K is the thermal expansion coefficient of steel and ΔT is the temperature change.

Another phenomenon observed in these strings is buckling, which leads to shortening. Mitchell [2] employs the helical buckling correlations for vertical wells proposed by Lubinski et al. [10]. In this context, the string undergoes a buckling strain ε_B and a contact force W_n , given by

$$\varepsilon_B = \begin{cases} 0 & F_f \leq 0 \\ -\frac{r_c^2}{4EI} F_f & F_f > 0 \end{cases}, \quad (3)$$

$$W_n = \begin{cases} 0 & F_f \leq 0 \\ -\frac{r_c}{4EI} F_f^2 & F_f > 0 \end{cases}, \quad (4)$$

with

$$F_f = -F_a + P_i A_i - P_o A_e, \quad (5)$$

where r_c is the annular radius, I is the moment of inertia of the string, F_f is the buckling force, P_i and A_i are the internal pressure and area, while P_o and A_e are the external pressure and area.

Based on these strains, one can define the axial strain as

$$\varepsilon_z = u' - \varepsilon_T - \varepsilon_B, \quad (6)$$

where u' is the total axial strain.

The solution to the thick-walled cylinder problem provides a relation for the stresses, allowing the axial force in eq. (1) to be defined as

$$F_a = EA_s(u' - \varepsilon_T - \varepsilon_B - \varepsilon_H), \quad (7)$$

with

$$\varepsilon_H = -\frac{2\nu}{EA_s}(P_i A_i - P_o A_e). \quad (8)$$

The strain ε_H relates to the poisson effect or ballooning in the strings. Lateral pressures from fluids inside and outside the string cause this effect. The tangential and radial stresses lead to contraction or expansion of the string, resulting in axial strains.

Substituting eq. (7) into the expression in Fig. 1 leads to the following equilibrium equation:

$$[EA_s(u' - \varepsilon_T - \varepsilon_B - \varepsilon_H)]' = -W_a \cos(\theta) \pm \mu W_n. \quad (9)$$

As detailed by Mitchell [2], the use of eq. (9) for friction analysis is necessary because it requires considering the direction of displacements u , and equation in Fig. 1 alone is not sufficient. In many operational scenarios involving tubing, boundary conditions related to displacements at the packer or the wellhead also exist. Thus, eq. (9) is used to determine displacements and eq. (7) to calculate axial forces. The axial and contact force due to buckling depend on the axial force, requiring an iterative approach in eq. (9).

When proposing an approximate displacement field, the solution to eq. (9) is not exact. One approach to determine the coefficients of this field and minimize the error from the approximation is to multiply the equilibrium equation by weighting functions W_j and then integrate over the element domain $[z_1, z_2]$. This technique is known as the weighted residual method, which, when associated with the Galerkin method, results in

$$\int_{z_1}^{z_2} \{ [EA_s(u'(z) - \varepsilon_T - \varepsilon_B - \varepsilon_H)]' - (-W_a \cos(\theta) \pm \mu W_n) \} \phi_j dz = 0. \quad (10)$$

where ϕ_j are the interpolating functions of the approximate displacement field $u(z)$, which is given by

$$u(z) = c_1 \phi_1(z) + c_2 \phi_2(z) + c_3 \phi_3(z) + c_4 \phi_4(z). \quad (11)$$

The coefficients c_j and the functions ϕ_j are based on the elements shown in Fig. 2, defined by the degrees of freedom presented in the image. Note that Mitchell [2] used a cubic element with 2 nodes, which has degrees of freedom for displacement and axial strain. In contrast, the other elements proposed in this work have degrees of freedom only for displacement.

Regarding the interpolating functions, they can be expressed as a function of a variable x , as indicated in eq. (12) and detailed in Tab. 1. This table also presents the stiffness matrix K_g and the force vector F for each element. The variables dx_j account for contributions from thermal deformations, buckling, and ballooning effects,

as well as friction force in the force vector, as shown in eq. (13). The element length is represented by λ , while F_{a1} and F_{a2} represent boundary force conditions at the top and bottom of the element, respectively.

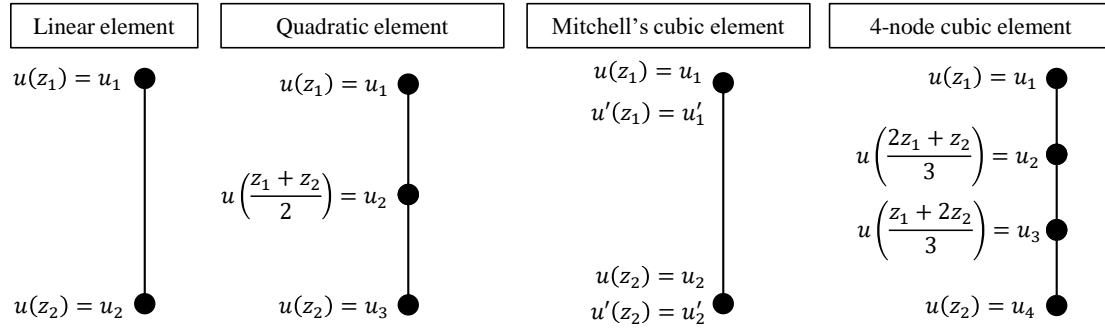


Figure 2. Finite elements for numerical axial analysis with friction in tubing strings.

$$x = \frac{2(z - z_1)}{(z_2 - z_1)} - 1. \quad (12)$$

$$dx_j = \int_{z_1}^{z_2} EA_s(\varepsilon_T + \varepsilon_B + \varepsilon_H)\phi'_j dz - \int_{z_1}^{z_2} \pm\mu(W_n + F_n)\phi_j dz. \quad (13)$$

Table 1. Interpolation functions, stiffness matrix, and force vector of the finite elements under study.

Elem.	Linear	Quadratic	Mitchell's cubic	4-node cubic
ϕ_1	$\frac{1}{2}(2 - x)$	$\frac{1}{2}(x^2 - x)$	$\frac{1}{4}(x^3 - 3x + 2)$	$\frac{1}{16}(-9x^3 + 9x^2 + x - 1)$
ϕ_2	$\frac{1}{2}(2 + x)$	$-x^2 + 1$	$\frac{1}{4}(x^3 - x^2 - x + 1)$	$\frac{1}{16}(27x^3 - 9x^2 - 27x + 9)$
ϕ_3	0	$\frac{1}{2}(x^2 + x)$	$\frac{1}{4}(-x^3 + 3x + 2)$	$\frac{1}{16}(-27x^3 - 9x^2 + 27x + 9)$
ϕ_4	0	0	$\frac{1}{4}(x^3 + x^2 - x - 1)$	$\frac{1}{16}(9x^3 + 9x^2 - x - 1)$
K_g	$\frac{EA_s}{\lambda} \begin{bmatrix} 1 & -1 \\ -1 & 1 \end{bmatrix}$	$\frac{EA_s}{\lambda} \begin{bmatrix} \frac{7}{3} & -\frac{8}{3} & \frac{1}{3} \\ -\frac{8}{3} & \frac{16}{3} & -\frac{8}{3} \\ \frac{1}{3} & -\frac{8}{3} & \frac{7}{3} \end{bmatrix}$	$EA_s \begin{bmatrix} \frac{6}{5\lambda} & \frac{1}{10} & -\frac{6}{5\lambda} & \frac{1}{10} \\ \frac{1}{10} & \frac{2}{15\lambda} & -\frac{1}{10} & -\frac{1}{30\lambda} \\ -\frac{6}{5\lambda} & -\frac{1}{10} & \frac{6}{5\lambda} & -\frac{1}{10} \\ \frac{1}{10} & -\frac{1}{30\lambda} & -\frac{1}{10} & \frac{2}{15\lambda} \end{bmatrix}$	$\frac{EA_s}{\lambda} \begin{bmatrix} \frac{37}{10} & -\frac{189}{40} & \frac{27}{20} & -\frac{13}{40} \\ -\frac{189}{40} & \frac{54}{5} & -\frac{297}{40} & \frac{27}{20} \\ \frac{27}{20} & -\frac{297}{40} & \frac{54}{5} & -\frac{189}{40} \\ -\frac{13}{40} & \frac{27}{20} & -\frac{189}{40} & \frac{37}{10} \end{bmatrix}$
F	$W_a\lambda \begin{bmatrix} \frac{1}{2} + dx_1 - F_{a1} \\ \frac{1}{2} + dx_2 + F_{a2} \end{bmatrix}$	$W_a\lambda \begin{bmatrix} \frac{1}{6} + dx_1 - F_{a1} \\ \frac{2}{3} + dx_2 \\ \frac{1}{6} + dx_3 + F_{a2} \end{bmatrix}$	$W_a\lambda \begin{bmatrix} \frac{1}{2} + dx_1 - F_{a1} \\ \frac{1}{12}\lambda + dx_2 \\ \frac{1}{2} + dx_3 \\ -\frac{1}{12}\lambda + dx_4 + F_{a2} \end{bmatrix}$	$W_a\lambda \begin{bmatrix} \frac{1}{8} + dx_1 - F_{a1} \\ \frac{3}{8} + dx_2 \\ \frac{5}{8} + dx_3 \\ \frac{1}{8} + dx_4 + F_{a2} \end{bmatrix}$

3 Computational implementation and verification of the numerical modelling of friction due to buckling

The computational implementation of the finite element numerical modelling follows the methodology presented in Rodrigues [9]. The only difference is that, instead of the cubic element used by Mitchell [2], this approach considers linear, quadratic, and cubic elements with 4 nodes, featuring the characteristics defined above.

To verify the computational implementation of the new elements, a tubing string from the vertical well presented in Lubinski et al. [10] is studied during a squeeze cementing operation, assuming a friction coefficient of 0.3. Mitchell [11] and Rodrigues [9] developed analytical solutions for axial forces and elastic displacements with friction in such scenario, which are used as reference solutions. The Python programming language is used on a personal computer with an Intel Core i5-10300U CPU 2.50 GHz, 4 cores, 8 logical processors, and 8 GB of RAM.

Figure 3 shows the percentage errors in displacements and forces from a mesh refinement study, comparing analytical solutions and the elements presented in this work. The first mesh is composed by four elements of equal length. Subsequently, the mesh is refined by halving the length of each element. The correct computational implementation of the models is evident from the convergence characteristics and the low error in forces and

displacements, which is less than 5%. The linear element is an exception, as it requires increased mesh refinement to meet this criterion.

In Figure 3(a), the percentage error in elastic displacement is lower for the 4-node cubic element. This is due to its higher number of displacement degrees of freedom. The quadratic element also performs comparably or even as well as the cubic element proposed by Mitchell [2], despite having a second-degree displacement function. For forces at the top of the tubing, as shown in Fig. 3(b), the element proposed by Mitchell [2] shows zero error. This result is expected because the example includes a packer seal bore, and the axial force at the tubing base is specified in the displacement degree of freedom of that element. Consequently, other models require more refinement to achieve the expected value, which is related to the non-linearity of the friction force and its occurrence in only a portion of the tubular. For the axial force at the top (see Fig. 3(c)) the 4-node cubic aligns more closely with the analytical solution, while the quadratic element and the Mitchell’s cubic element exhibit similar behavior.

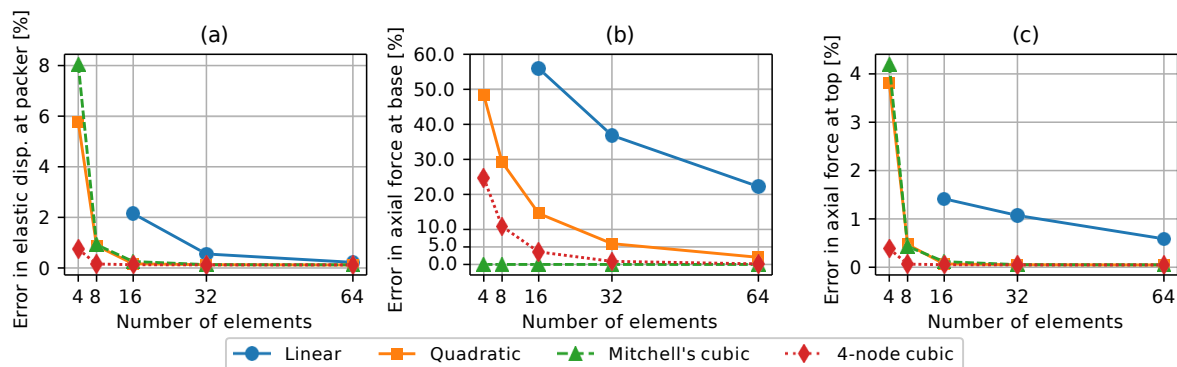


Figure 3. Verification of finite element modelling through mesh refinement study in tubing string.

4 Case study

A realistic synthetic vertical well is studied. This well is of offshore nature and the water depth is 1957 m. The sections of the tubing are in Tab. 2, and additional well informations can be found in Rodrigues [9].

Table 2. Sections and properties of the tubing in the vertical well.

Section	Measure Depth [m]		Tubular		
	Top	Base	OD (in) [mm]	ID (in) [mm]	W_a (lbf/ft) [kN/m]
1	1976.27	1992.62	(5.5) [140]	(4.67) [119]	(23) [0.336]
2	1992.62	2446.96	(6.625) [168]	(5.791) [147]	(28) [0.409]
3	2446.96	2492.24	(5.5) [140]	(4.67) [119]	(23) [0.336]
4	2492.24	5261.79	(6.625) [168]	(5.791) [147]	(28) [0.409]
5	5261.79	5352.50	(5.5) [140]	(4.67) [119]	(23) [0.336]
6	5352.50	5375.00	(4.5) [114]	(3.92) [100]	(13.5) [0.197]

The packer in the tubing is located at a measured depth of 5375 m and is mechanically set. Thus, the tubing is fixed, rather than being free at one end as in the previous example. The tubing is evaluated during a production operation. Fig. 4(a) and 4(b) show the pressures and temperatures during this operation.

Similarly to the previous example, a mesh study is realized by refining the elements along each section of the tubing. However, since the errors in this example are bigger away from the top and bottom, the maximum absolute error along the tubular is used as the error metric. Additionally, because no analytical solution is available for this case, the modelling proposed by Mitchell [2] with a very refined mesh is used as the reference for the axial forces in this study. Thus, the strategy of using small elements at discontinuities is employed to compare the element proposed by Mitchell [2] with the elements proposed in this work.

Figure 5 illustrates the maximum absolute error in axial forces and the computational cost in the analysis of a fixed tubing during production, considering the studied elements. The analysis with the linear element is not presented due to the need for more refined meshes. In Fig. 5(a), it can be observed that the maximum absolute errors between the proposed cubic element and the reference element are similar, with the proposed one

being slightly more accurate. This result is expected since, in this example, there is no prescribed axial force and all degrees of freedom of the 4-node cubic element are related to displacement. The maximum errors are around 2 klbf [8,896 kN], while the forces range between 150 klbf [667,233 kN] and -120 klbf [-533,787 kN], indicating the accuracy of the 4-node cubic element. The quadratic element shows larger errors, but these decrease significantly with mesh refinement. Regarding computational cost, as illustrated in Fig. 5(b), the simulations take seconds, and the quadratic element has the lowest computational cost due to its fewer degrees of freedom.

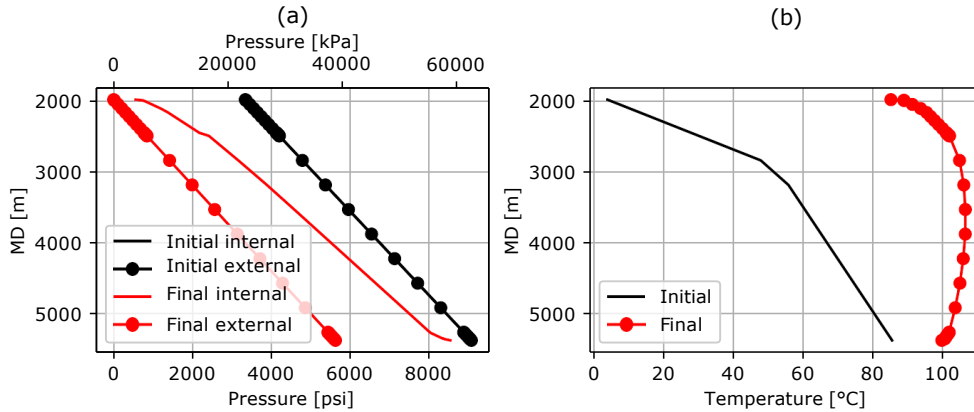


Figure 4. Pressures and temperature in tubing during production.

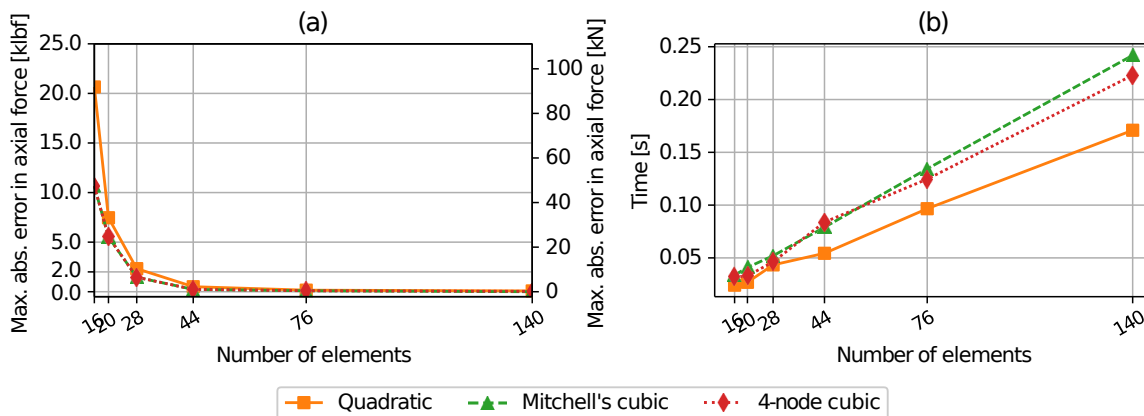


Figure 5. Mesh refinement study using different elements in fixed tubing.

The Figure 6 illustrates the axial forces in the tubing using a mesh with 140 elements. As can be observed, the quadratic and cubic 4-node elements show no noise in the depths with diameter variation (see Tab. 2). This characteristic represents an advantage for the proposed elements. They can also exhibit errors similar to the reference model with a lower computational cost, as is the case for the quadratic element.

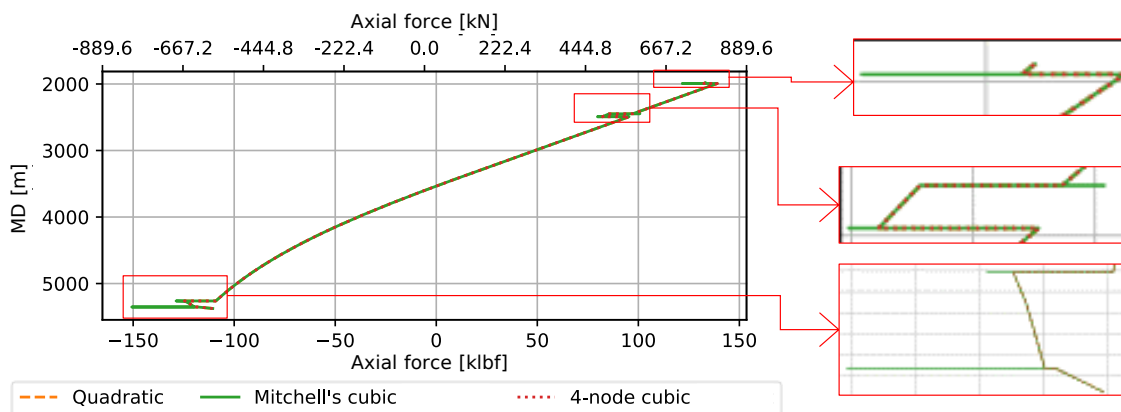


Figure 6. Axial forces in fixed tubing under production.

5 Conclusions

A finite element model for predicting axial forces with friction in tubing under operational loads with linear, quadratic, and cubic displacements was implemented and correctly verified through analytical solutions. In the case study with a fixed tubing, the quadratic element demonstrated the best cost-benefit ratio with meshes of 44 elements. The error in the axial forces was similar to that of cubic models but with a lower computational cost, which is relevant for real-time analysis in industry. Additionally, no noise in the axial forces was observed in relation to the element proposed by Mitchell [2]. The next steps of this work include simulating additional wells, including directional ones, to more precisely discuss the applicability of the proposed elements.

Acknowledgements. The authors would like to thank PETROBRAS for the financial and technical support related to the development of the research project “Desenvolvimento de ferramentas computacionais para modelagem em tempo real da integridade de estrutura de poço” (ANP code 23599-4).

Authorship statement. The authors hereby confirm that they are the sole liable persons responsible for the authorship of this work, and that all material that has been herein included as part of the present paper is either the property (and authorship) of the authors, or has the permission of the owners to be included here.

References

- [1] J. Bellarby. Chapter 9 Tubing Stress Analysis. In J. Bellarby, ed, *Well Completion Design*, volume 56 of *Developments in Petroleum Science*, pp. 473–556. Elsevier, 2009.
- [2] R. F. Mitchell. Comprehensive Analysis of Buckling With Friction. *SPE Drilling & Completion*, vol. 11, n. 03, pp. 178–184, 1996.
- [3] R. F. Mitchell. The Effect of Friction on Initial Buckling of Tubing and Flowlines. *SPE Drilling & Completion*, vol. 22, n. 02, pp. 112–118, 2007.
- [4] R. F. Mitchell. Tubing Buckling—The State of the Art. *SPE Drilling & Completion*, vol. 23, n. 04, pp. 361–370, 2008.
- [5] J. F. Brett, A. D. Beckett, C. A. Holt, and D. L. Smith. Uses and Limitations of a Drillstring Tension and Torque Model To Monitor Hole Conditions. volume All Days of *SPE Annual Technical Conference and Exhibition*. SPE-16664-MS, 1987.
- [6] J. Wu and H. C. Juvkam-Wold. Helical buckling of pipes in extended reach and horizontal wells part 2. *Journal of Energy Resources Technology, Transactions of the ASME*, vol. 115, n. 3, pp. 196–201, 1993.
- [7] S. Miska, W. Qiu, L. Volk, and J. Cunha. An improved analysis of axial force along coiled tubing in inclined/horizontal wellbores. volume All Days of *SPE/CIM International Conference on Horizontal Well Technology*. SPE-37056-MS, 1996.
- [8] R. F. Mitchell, A. R. McSpadden, M. A. Goodman, R. Trevisan, R. D. Watts, and N. R. Zwarich. A Dynamic Model with Friction for Comprehensive Tubular-Stress Analysis. *SPE Drilling & Completion*, vol. 35, n. 03, pp. 369–381, 2020.
- [9] O. B. A. Rodrigues. Contribuição do atrito nos esforços axiais de colunas de produção e injeção em poços de petróleo submetidos a carregamentos operacionais. Master’s thesis, Universidade Federal de Alagoas, 2024.
- [10] A. Lubinski, W. Althouse, and J. L. Logan. Helical Buckling of Tubing Sealed in Packers. *Journal of Petroleum Technology*, vol. 14, n. 06, pp. 655–670, 1962.
- [11] R. F. Mitchell. Simple Frictional Analysis of Helical Buckling of Tubing. *SPE Drilling Engineering*, vol. 1, n. 06, pp. 457–465, 1986.